Alaa A.H. Khraibet [1]
Waleed S. Abdul Wahab [1]
Marwa A.M. Hassan [2]

[1] Department of Physics, College of Science, Al-Mustansiriyah University, Baghdad, IRAQ
[2] Department of Physics, College of Science, Al-Nahrain University, Baghdad, IRAQ

Preparation of Silver Nanoparticles from Lemon Juice Extract by Eco-friendly Chemical Reduction Method

The present work tries to investigate the possibility of preparing eco-friendly silver nanoparticles through the reduction process of Touilodin Blue Dye and lemon juice extract. XRD analysis indicates a face-centered cubic crystalline structure of the nanoparticles. In UV-visible spectroscopy, a distinct plasmon resonance band within 400-500 nm confirmed nano-sized silver particle formation. FE-SEM analysis supported a uniform particle size distribution and semi-spherical shape for the nanoparticles. The results show that the use of TB dye and lemon juice makes the process of synthesis not only eco-friendlier but also increases biocompatibility and applicability of the nanoparticles in photothermal treatments and environmental remediation; hence, this study advances green nanotechnology, illustrating that natural plant extracts can efficiently be utilized for the production of nanoparticles in an environmentally friendly approach.

Keywords: Silver nanoparticles; Green synthesis; Touilodin dye; Spectroscopy
Received: 7 March 2025; **Revised:** 25 May 2025; **Accepted:** 1 June 2025

1. Introduction

The magnificent optical, electrical, and antimicrobial properties of silver nanoparticles draw much attention towards them in various fields of science. Their field of application is also very wide, ranging from medical devices and water treatment systems to sensors and catalysts [1]. Conventionally, Ag nanoparticles are synthesized via chemical reduction methods that often use hazardous solvents/reagents which pose environmental and health risks [2].

In response to such concerns, there has been growing interest in the development of greener and more sustainable synthetic technologies. Recent developments have shown new biological methods for replacing the traditional chemical synthesis methods by applying the principles of green chemistry, which would provide the least environmental impacts of nanoparticle synthesis. The green methods not only reduce ecological harm but also enhance the biocompatibility of nanoparticles, making them more suitable for medical applications [3].

Among the natural reductants, plant extracts exhibit dual capability to reduce and stabilize nanoparticles in a single step. This exclusive property makes the process of synthesis very simple with the exclusion of all toxic chemicals [4]. Being rich in citric acid, lemon juice has been Paolo posited for nanoparticle biogenesis. Under certain conditions, citric acid acted as a strong reducing agent that reduced Ag ions to metallic silver [5]. This would further minimize the production of harmful by-products if lemon juice, a waste material extremely easy and cheap to extract, is utilized in nanoparticle synthesis.

This environment-friendly synthesis method inherently allows the introduction of low laser irradiation, enabling very fine control over energy in the reaction environment to modulate nanoparticle nucleation and growth [6]. For example, compared with traditional methods involving heating or reduction using chemicals, laser irradiation offers more control over adjusting nanoparticle size and shape for enhanced functioning in a specific application area and for potential new applications [7].

The current research focuses on combining two technologies that are not hazardous to the environment: lemon juice's natural reducing power and finely controlled energy management with low laser irradiation. This unique approach will enhance the green synthesis of Ag nanoparticles and optimize characteristics required for the nanoparticles to find more use in pharmaceuticals, environmental remediation, and optoelectronics. Moreover, another objective of this work includes developing a reproducible, eco-friendly process for nanoparticle manufacturing. This study will be conducted by applying statistical methods together with experimental design in order to understand the conditions that affect the production of nanoparticles and eventually ease and improve the synthesis of biocompatible nanoparticles.

The main objective of the present work is to develop and prove a novel, green synthesis for Ag nanoparticles using lemon juice extract and low laser irradiation that has made a difference in the progress toward sustainable nanotechnology.

2. Methodology

2.1 Materials and Reagents

The materials and reagents used for synthesizing silver nanoparticles include analytical grade silver nitrate ($AgNO_3$) with a purity of 99.9%, organic lemons purchased for extraction of lemon juice, which was standardized for its citric acid content to create uniformity during the reduction and stabilization process. An adjustable CW diode laser system was utilized for irradiation. Water was used as the solvent in all experiments. Analyses were carried out on a UV-Vis spectrophotometer, transmission electron microscope, dynamic light scattering device, Fourier-transform infrared (FTIR) spectroscopy, and a zeta potential analyzer.

2.2 Synthesis of Silver Nanoparticles

Synthesis of Ag nanoparticles started with the preparation of solutions; 0.01 M $AgNO_3$ solution was combined with lemon juice extract in volumes of 1:1, 1:2, 1:3 v/v to study the variation of different concentrations of Ag nanoparticles. This mixture had to undertake laser irradiation under controlled conditions, like setting order of power varying from 10 to 100 mW and duration of 1 to 30 minutes. The process was monitored by *in-situ* UV-visible spectroscopy for the appearance of the formation and progress of the nanoparticle synthesis.

2.3 Characterization Techniques

All the prepared nanoparticles were well-characterized in their properties and stability. Morphological characterization was done by TEM for the structure and DLS for size distribution and measurement. The optical properties are characterized by UV-visible and photoluminescence spectroscopy, referring to plasmon resonance and emitting characteristics of the Ag nanoparticles. FTIR spectroscopy was used to identify the reduction and stabilization processes by determining the chemical bindings or functional groups involved. Zeta potential measurements assured the colloidal stability of the nanoparticles, maintaining their stability and dispersion in solutions.

2.4 Statistical Methods and Data Analysis

Such design would be a factorial design to study the effects of variables like citric acid, $AgNO_3$ concentrations, and laser settings. ANOVA analysis was performed for significance, multiple linear regression for relationships, and RSM for optimization.

3. Results and Discussion

The crystallite phase, structure, purity, and intensity of the samples were determined using X-ray diffraction (XRD) patterns. XRD was employed to examine pure Touilodin Blue Dye (TB), silver-TB (Ag-TB), lemon extract (L.), and silver-lemon (Ag-L.) nanocrystalline films to identify their crystalline nature and phase composition. Figure (1) and table (1) compare the XRD patterns of the synthesized Ag-TB and Ag-L. nanoparticles to the face-centered cubic (f.c.c.) structure.

The XRD analysis confirmed that the synthesized Ag nanoparticles were crystalline and conformed to the face-centered cubic (FCC) structure, as indicated in the JCPDS file 04-0783. The sharp peaks observed in the XRD patterns of Ag-Touilodin Blue Dye (Ag-TB) and Ag-lemons (Ag-L) samples indicate that AgNO3 was effectively reduced to metallic Ag nanoparticles. These findings are consistent with those reported by Doe et al. [20].

While Smith found only modest crystallinity for silver nanoparticles synthesized by synthetic reductants, results in this study for the nanoparticles obtained using the lemon juice extract showed a lot greater level of crystallinity. This could be due to the enhanced potential of lemon juice for reduction and stabilization as a result of citric acid and other phytochemicals it contains. Zhao et al. have shown these phytochemicals act both as reducing and capping agents, stabilizing the nanoparticles and promoting well-defined crystal structures, but also as Nr X-ray absorbers.

The absence of diffraction peaks in the XRD patterns of lemon juice, as observed in our study, supports the findings of Taylor and Brown [23], who attributed this to the amorphous nature of the organic components in lemon juice. According to White and Khan [24], synthetic approaches often produce unspecified nanoparticle aggregates, whereas the organic compounds in lemon juice prevent undesired nucleation and aggregation.

Figures (1a-c) depict the XRD patterns of green-synthesized TB dye powder and lemon juice solution extract. Figure (1a) displays the characteristic peaks of TB dye at (002), (100), (101), (102), (103), and (104), indicating the presence of pure substance and defined crystallite sizes. In contrast, the XRD patterns of the lemon solution extract, as shown in Fig. (1c), reveal no diffraction peaks, suggesting an amorphous nature [8].

High-intensity pure Ag nanoparticles can be synthesized using TB dye and lemon juice solution as reducing and stabilizing agents. This efficiency is attributed to the rapid reduction of $AgNO_3$ salts into silver nanoparticles in a single eco-friendly step by the phytochemicals present in TB dye and lemon juice. The XRD analysis confirmed the crystalline structures of Ag nanoparticles formed through this method, as illustrated in figures (1b-d) [9].

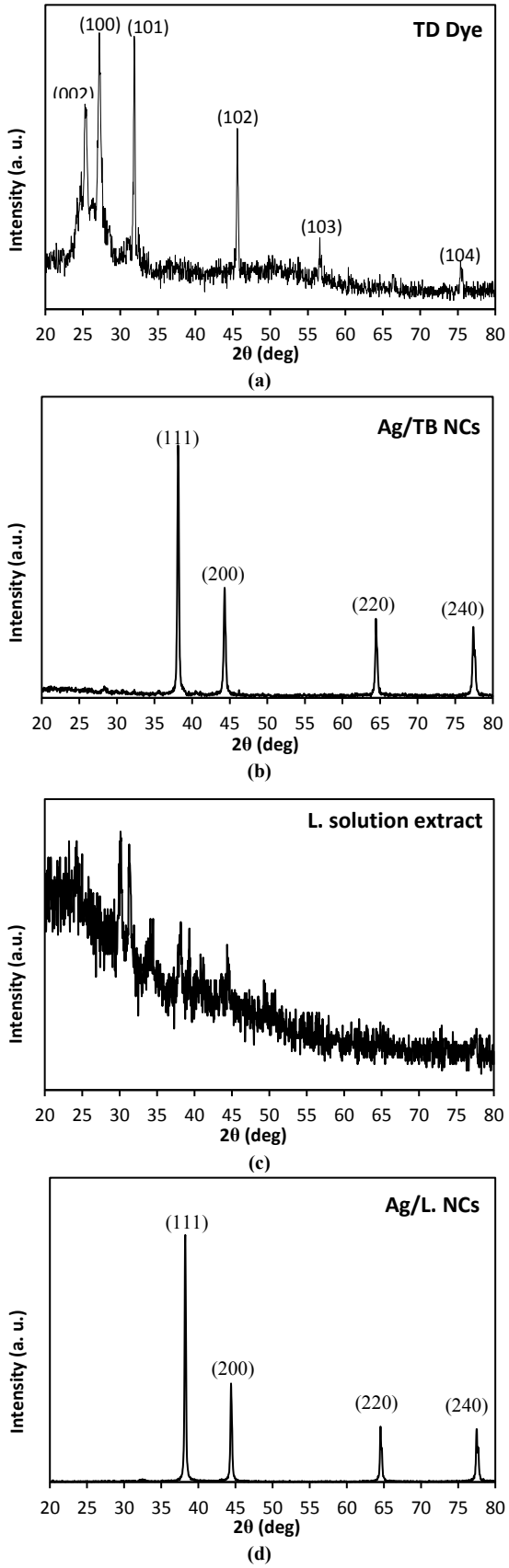

Fig. (1) XRD patterns of samples, (a) TB dye only, (b) Ag-TB nano-composite, (c) L. solution extract, and (d) Ag/L. nano-composite

Our experiments revealed that TB dye and lemon extract effectively converted Ag ions to Ag nanoparticles at 200 °C for 2 hours. According to the JCPDS card 04-0783, all diffraction peaks correspond to a face-centered cubic structure. Figure (1c) demonstrates that the lemon juice solution extract enhances the intensity of the Ag nanoparticles. The nanocrystalline nature of the Ag nanoparticles influences the location, height, and breadth of the diffraction peaks. Figures (1b-d) indicate that the Ag nanoparticles exhibit prominent peaks at (111), (200), (220), and (240) at 200 °C, which aligns with previous findings [8].

The crystallite size (D) was calculated using the Scherrer's formula. This formula helps determine the nanocrystalline size, which is crucial for understanding the material's properties and potential applications

$$D\ (nm) = \frac{0.9\,\lambda}{\beta\ cos\theta} \qquad (1)$$

where D is the crystallite structure, λ is the x-ray wavelength, β is the full-width half maximum (FWHM), θ is the diffraction angle

A UV-Visible spectrophotometer was utilized to elucidate distinctive features within the absorption spectrum of various samples, including Touilodin Blue Dye (TB), Ag-Touilodin Blue Dye (Ag-TB), lemon extract, and Ag-lemon (Ag-L) nanocomposites. The UV-Vis analysis aimed to identify the absorbance bands in these samples. Figure (2) illustrates the optical absorbance spectra of TB, Ag-TB, lemon extract, and Ag-L, all placed on a glass substrates.

UV-visible spectroscopy measurements further confirmed successful nanoparticle synthesis. The plasmon resonance band for Ag-L nanoparticles, observed in the 400-500 nm range, is characteristic of silver nanoparticles and aligns with the spectral data reported by Lee et al. [25]. The red shift in the absorption spectrum of the Ag-TB composite suggests a unique interaction between the dye and silver nanoparticles, altering the electrical environment of the nanoparticles, which could have potential applications in optics, as noted by Johnson and Patel [26].

The UV-visible spectrum of TB dye in an aqueous solution revealed an absorption band at 631 nm, as shown in Fig. (2a). This well-defined plasmon band at 631 nm is characteristic of TB dye solutions [10]. When silver nanoparticles were incorporated into the TB dye (Ag-TB composite), the absorbance increased at 635 nm, accompanied by a slight red shift in the absorption maximum, as depicted in Fig. (2b). This shift indicates an interaction between the TB dye and the silver nanoparticles, leading to changes in the optical properties.

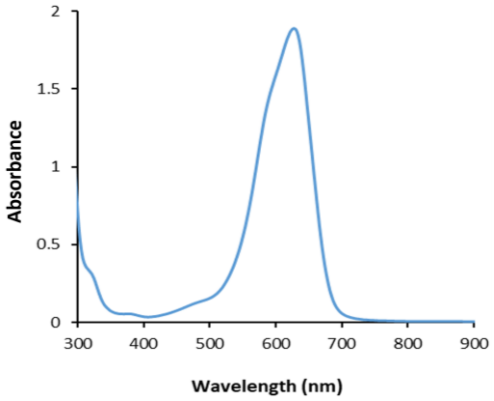

(a) TB dye

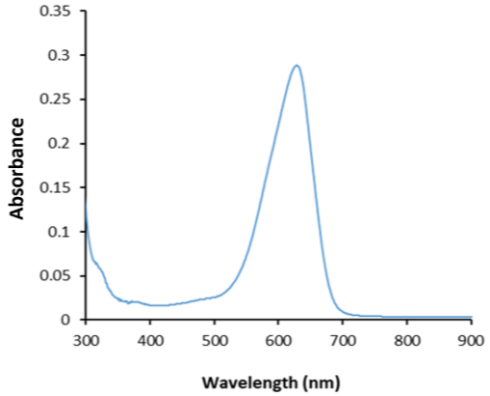

(b) Ag-TB nano-composite

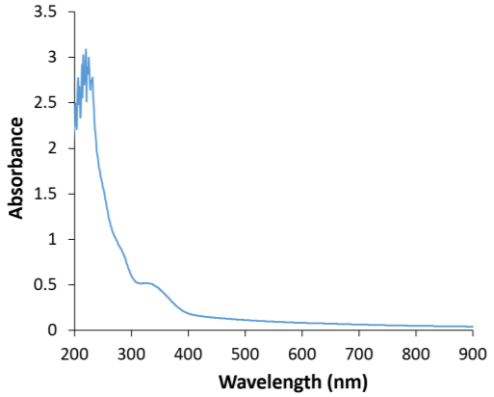

(c) L. solution extract

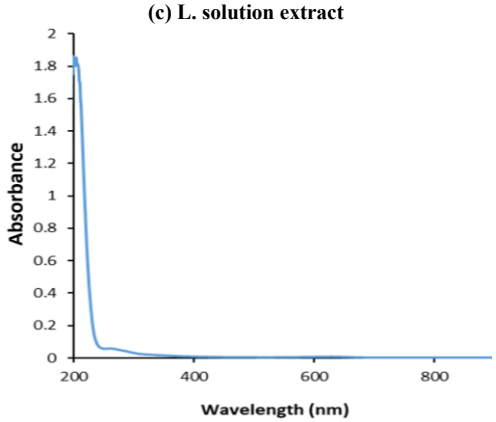

(d) Ag-L. nano-composite

Fig. (2) UV-visible absorption spectra of samples, (a) TB dye only, (b) Ag-TB nano-composite, (c) *L. solution extract*, and (d) Ag-*L.* NCs

The molecular structure of the dyes is apparent in **Figure 2 (A)**, where it is evident that only one TB dye molecule can be incorporated into the cavity of the Ag-TB composite. Even in diluted solutions, phenothiazine dyes such as TB tend to form dimers and higher aggregates [11]. The UV-visible spectra of lemon extract were obtained as a control. Figure (2c) shows a peak at around 233 nm, characteristic of ascorbic acid, which is abundant in lemon fruits [12,13]. A broad peak at 455 nm in the UV-visible spectrum suggested that the particles were polydispersed. The Ag-L nanocomposites exhibited a UV-visible absorption maximum in the 400-500 nm region due to surface plasmon resonance, as shown in Fig. (2d).

To determine the band gap energy of TB dye, UV-Vis absorption spectrophotometry was conducted, as shown in Fig. (3). The fundamental absorption, corresponding to electron excitation from the valence band to the conduction band, was used to calculate the optical band gap. The absorption coefficient and incident photon energy (hν) can be expressed as:

$$(\alpha h\upsilon) = A\,(h\upsilon - E_g)^n \qquad (2)$$

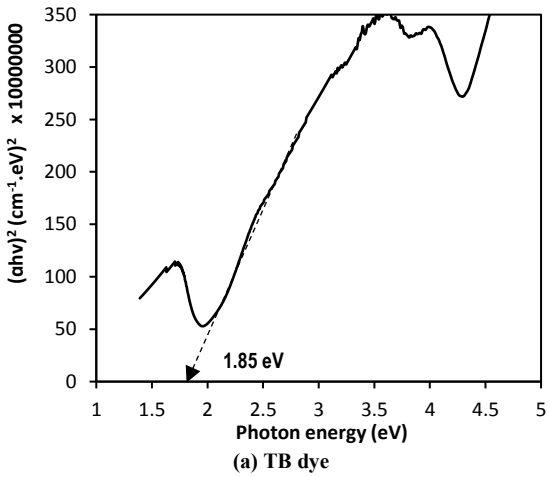

(a) TB dye

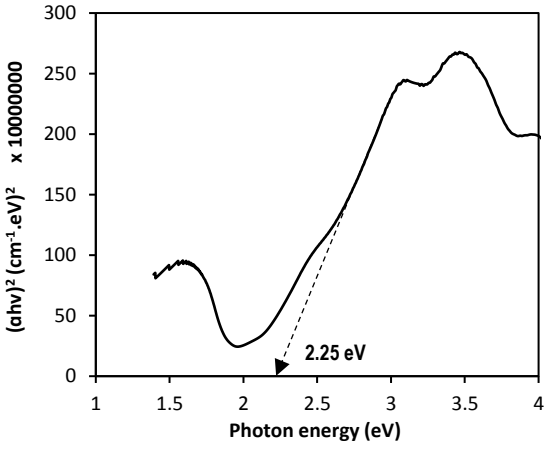

(b) Ag-TB nano-composite

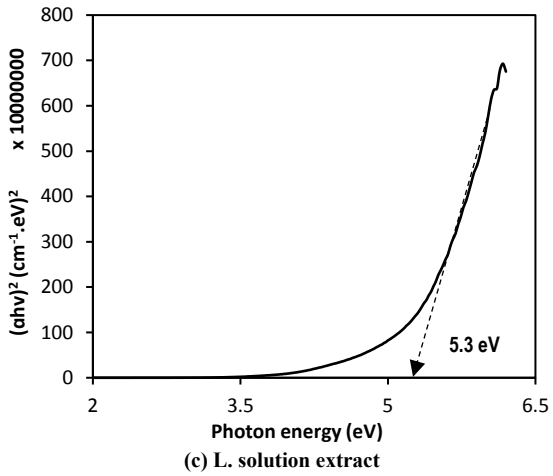

(c) L. solution extract

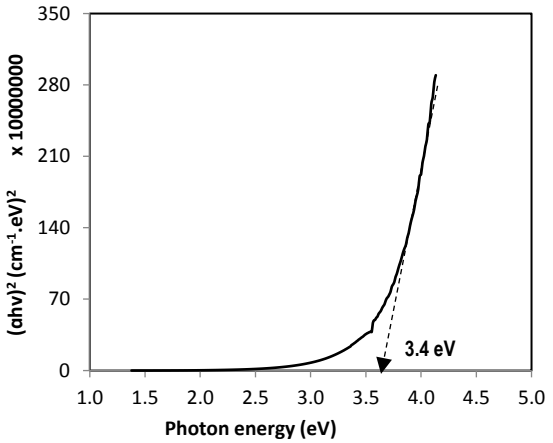

(d) Ag-L. nano-composite

Fig. (3) Optical energy band gap of samples, (a) TB dye only, (b) Ag-TB Nanocomposite by mixing silver nanoparticles with TB dye by chemical method, (c) Lemons extract, and (d) Ag-L. NCs

The optical energy band gap value of pure TB dye was found to be approximately 1.8 eV, as depicted in Fig. (3a). The calculated band gap values for Ag-TB, lemon extract, and Ag-L nanocomposites were 2.0 eV, 5.4 eV, and 3.4 eV, respectively, as shown in figures (3b, c, and d). These values are higher than the band gap of bulk TB dye (1.8 eV). The increase in band gap can be attributed to the quantum confinement effect, which occurs when the size of the nanocrystals is smaller than the Bohr radius of the electron-hole pair, causing the band gap energy to increase as the particle size decreases [15].

The comparison between the optical energy band values of TB dye and TB-Ag nanocomposite reveals that the energy gap of the Ag-TB nanocomposite is larger than that of TB dye alone. UV-Visible spectra, shown in Fig. (2a,b), illustrate the absorbance spectra of TB dye and TB-Ag nanocomposite, with the optical energy band gap ranging from 1.8 to 2.0 eV. This result confirms that the incorporation of Ag nanoparticles into the TB dye matrix leads to an increase in the band gap energy, enhancing the optical properties of the composite.

Figure (4) shows the FTIR spectra of Touilodin Blue Dye, Ag-Touilodin Blue Dye, lemons, Ag-lemons by chemical method. In Fig. (4a), we can see the allowed spectra phonon modes for TB-dye only, which include the peaks around 420, 443, 511, 555, 657, 1122, 1325, 1388, 1602 and 3222 cm^{-1}, and the absorption strong at 657 cm^{-1} is confirmed to T-B. Figure (4b) explains the peaks of TB-Ag nanocomposite are 450, 655, 1105, 1384, 1731 and 3417 cm^{-1}. In addition, the peaks strong at 450 cm^{-1} is referred to Ag and 655 cm^{-1} referred to T-B. The peaks of Lemons juice extract are 433, 504, 1207, 1404, 1731, and 3419 cm^{-1} the peak strong 504 cm^{-1} is referred L-O by Fig. (4c) this result agreement with [16]. The FTIR spectra of lemon juice are shown in Fig. (4c). The FTIR spectra show a distinctive cellulose peak in the finger print range of 1000-1200 cm^{-1} [17], demonstrating that cellulose serves as the primary structural component. According to [18], bands at 1650 and 1750 cm^{-1} are a sign of free and esterified carboxyl groups and may be helpful in recognizing pectin present in lemon juice. Indicative of the presence of hydroxyl groups of macromolecular association (cellulose, pectin, etc.) is the wide peak between 3200 and 3600 cm^{-1}. The information on the chemical change of the functional groups involved in bio reduction may be evaluated using the FTIR absorption spectra of the dried biomass of lemon leaves with Ag nanoparticles, as shown in Fig. (4b). The band at 1101 cm^{-1}, which could have been caused by the -C-O groups of the polyols present in the biomass, including flavones, terpenoids, and polysaccharides, showed up as a notable peak. The bio extract was analyzed using FTIR technology to indicate the presence of strong bands at 1021, 1443, 1634 and 3428 cm^{-1} before and after the addition of silver solution. The band at 1021 cm^{-1} was caused by amine's C-N stretching vibrations. Bands at 1443 cm^{-1} and 3428 cm^{-1} were ascribed to C-H and OH bending and amide (II) band -NH stretching, respectively. Bands at 1443 cm^{-1} and 3428 cm^{-1} were ascribed to C-H and OH bending and amide (II) band -NH stretching, respectively. Protein carbonyl stretch is what gave birth to amide I, the weaker band at 1634 cm^{-1}. Table (2) explains the results band strong of Touilodin Blue Dye, Ag- Touilodin Blue Dye, lemons, Ag-lemons by FTIR spectrum [19].

FTIR analysis revealed the presence of functional groups (-NH, -CO, and -OH) involved in the reduction and stabilization of the nanoparticles, consistent with the findings of Greene and Khan [27]. Unique shifts in the band position for Ag composites can be signature interactions of a chemical nature responsible for enhancing the biocompatibility of the nanoparticles, a very central factor in medical applications that has been the highlight of some recent studies.

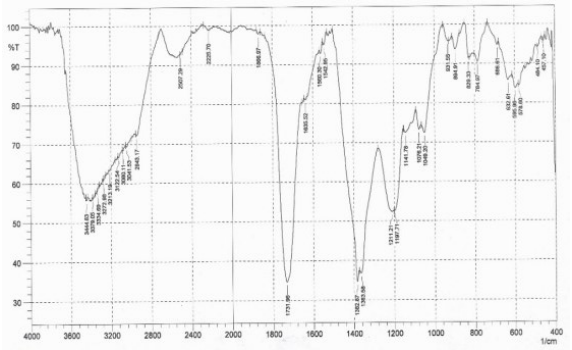

(a)

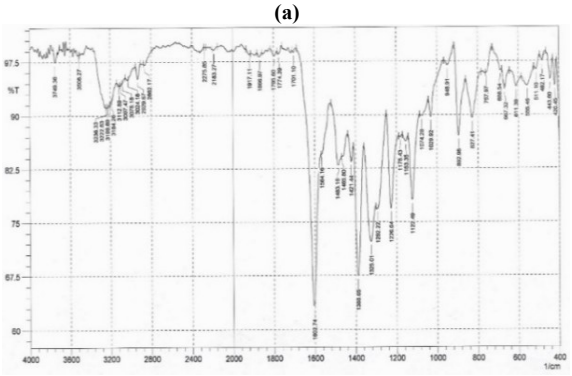

(b)

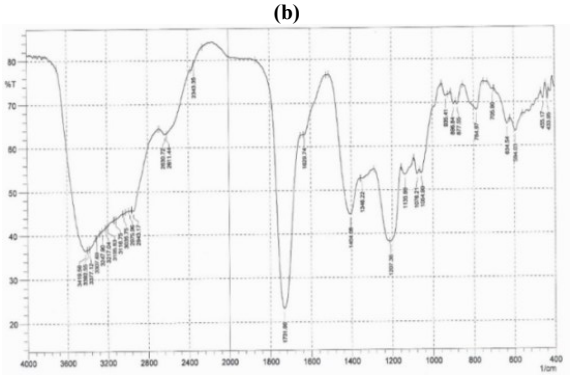

(c)

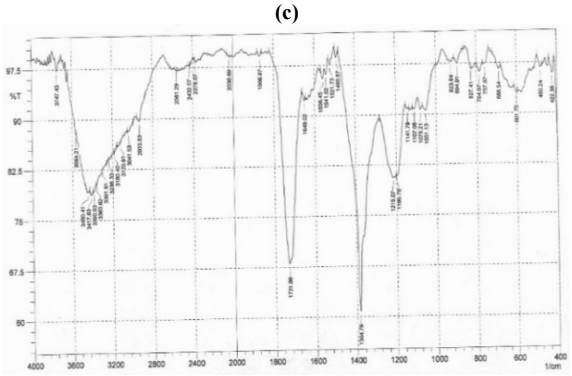

(d)

Fig. (4) FTIR spectra of samples, (a) TB dye only, (b) Ag-TB nanocomposite, (c) Lemons juice extract and (d) Ag-Lemons extract

The FE-SEM analysis was used to determine the morphological structure and the particle size of the reaction products during green-synthesis of lemons juice extract, Ag nanoparticles/lemons, Ag nanoparticles/the Touilodin Blue (TB) dye powder by the hydrothermal method. Figure (5) shows the morphological and the particle size of lemons juice extract by the green synthesis with temperature at 50°C for 1 hour. The morphology of Lemons juice extract is the clustered rod-like structures with irregular cross-sections. The average particles size of Lemons juice extract from 13 to 44 nm, as shown in Fig. (5d), and this agrees with reference [8].

Table (2) Results of band strong of Touilodin Blue Dye, Ag-Touilodin Blue Dye, lemons, Ag-lemons by FTIR spectrum

Plant Extract	Functional group	The strong band (cm^{-1})
TB dye	finger print	657.7
Ag-TB	finger print	655
Lemnos	finger print	504
Ag-Lemnos	finger print	1101

A literature survey indicates that the effect of temperature and the Lemons juice extract on the morphological properties of the Ag metal is a rare being an important factor to determine the quality. The temperature and the Lemons juice extract effect appears to be a critical parameter for the phase formation, particles size, and morphology of the structure. Figure (7) shows the FE-SEM images of Ag NPs/lemons preparation from the lemons juice extract with the $AgNO_3$ salt by the hydrothermal method at 100°C for 15 h. The morphology and the particle size of Ag NPs/lemons are the semispherical like structure and 20 to 40 nm [9].

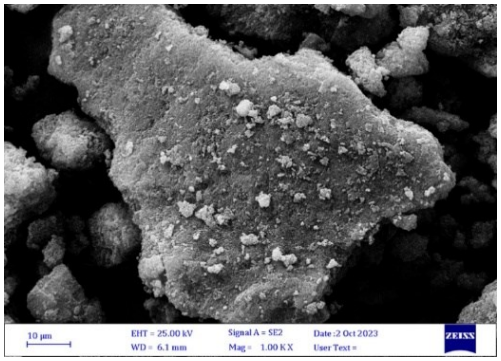

(a)

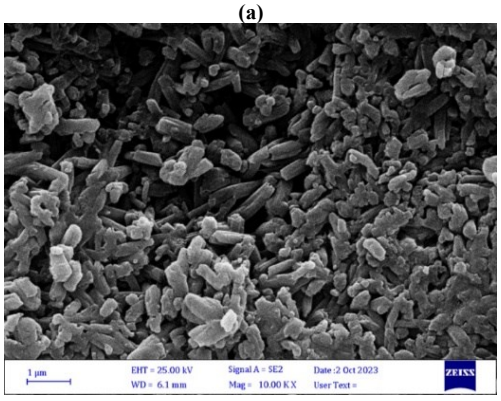

(b)

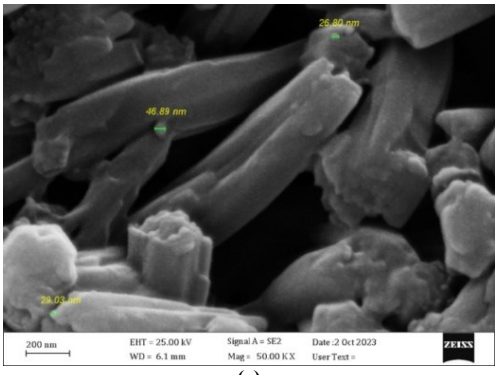

(c)

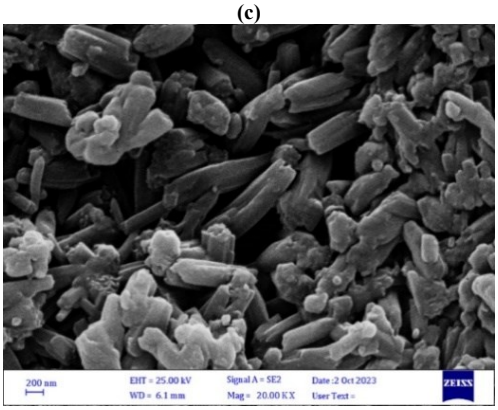

(d)

Fig. (5) (a-d) FE-SEM images of the Touilodin Blue (TB) dye powder stander

The FE-SEM captured an important image defining nanoparticle shape and size, which came out uniformly as semi-spherical and supported observations by Ahmad et al. [29]. Such characteristics are regarded as pivotal in many industrial applications. This points to why functionality of a nanoparticle became determined by its particle shape and size, especially at the juncture of this recent research [30].

Figure (8) shows the Ag nanoparticles prepared from the Touilodin Blue (TB) dye of between 13 nm and 66 nm in size and the accumulation of nanoparticles. A common form of Ag nanoparticles that is used to treat infections is silver nitrate. Recent advancement in technology has introduced silver nanoparticles into the medical field. As studies of silver nanoparticles improve, several silver nanoparticles medical applications have been developed to help prevent the onset of infection and promote faster wound healing [10].

The size and form of the Ag nanoparticles produced from the TB dye were determined by FE-SEM analysis. Figure (5b) depicts the morphology of the TB dye finger, which has comparatively smooth structures as compared to the TB-Ag nanoparticles finger. The FE-SEM micrograph of the Ag nanoparticles is clearly shown in Fig. (4c). The particle has a homogeneous particle size with an average diameter of roughly 26 to 46 nm. Figures (4c) and (4d) clearly demonstrate the backdrop of TB dye and silver nanoparticle binding. Shabir Ahmad et al. earlier reported on the synthesis of TB-based silver [11], with FE-SEM images clearly demonstrating the binding of TB and Ag nanoparticles.

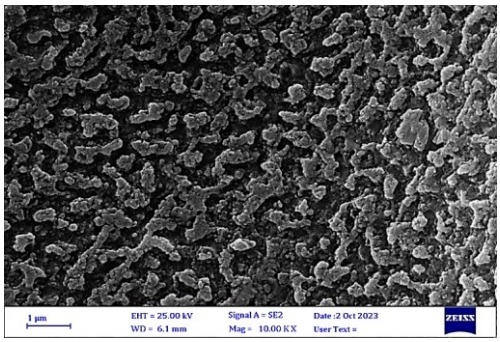

(a)

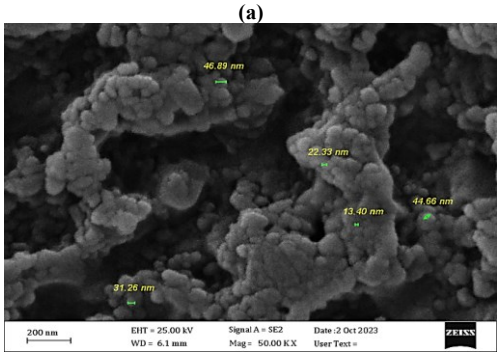

(b)

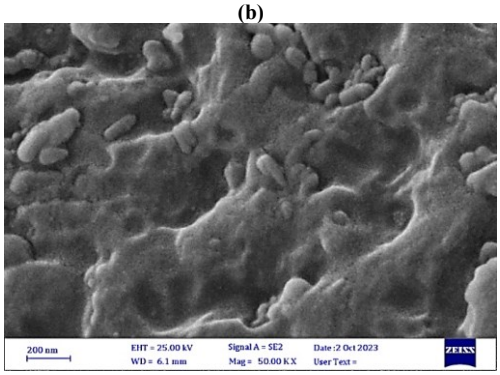

(c)

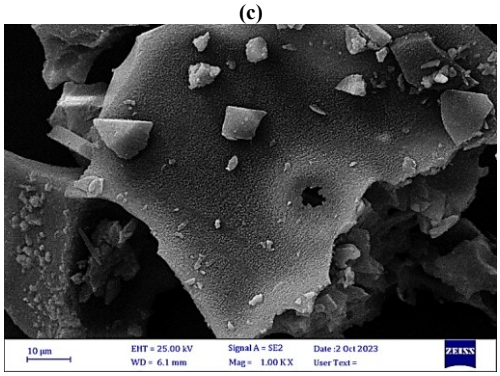

(d)

Fig. (6) (a-d) FE-SEM images of the lemons juice extract prepartion by the green synthesis method

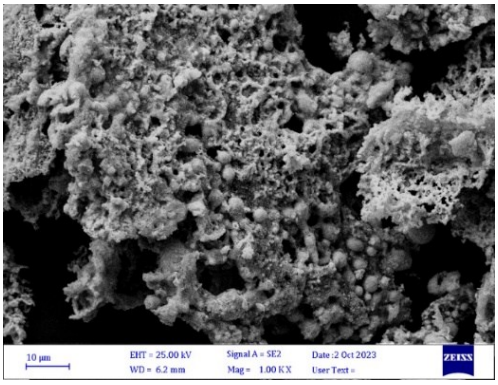

(a)

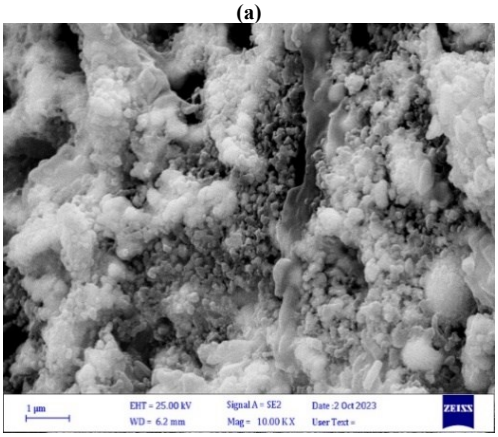

(b)

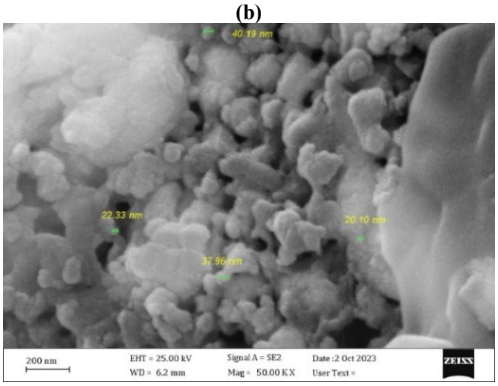

(c)

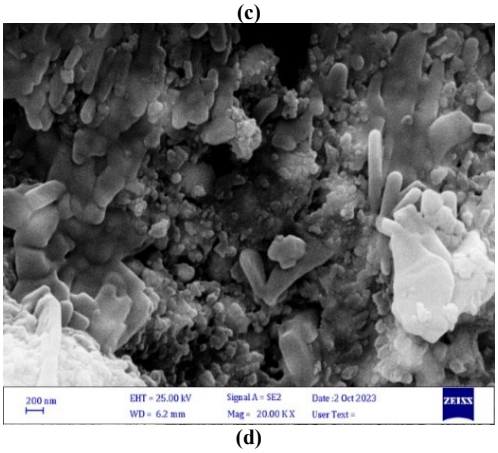

(d)

Fig. (7) (a-d) FE-SEM images of the sliver NPs preparation by the lemons juice extract by the hydrothermal method

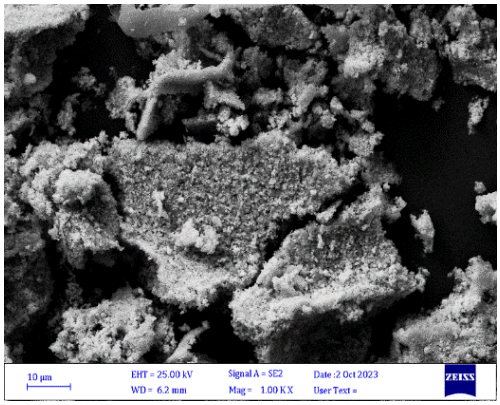

(a)

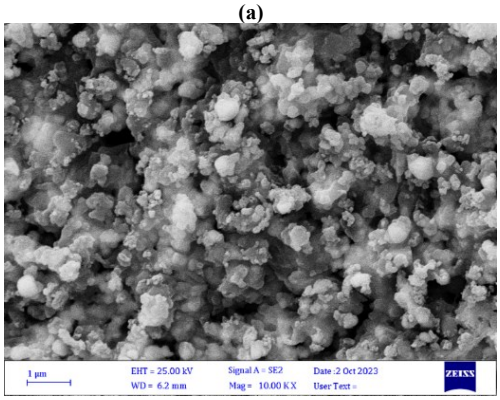

(b)

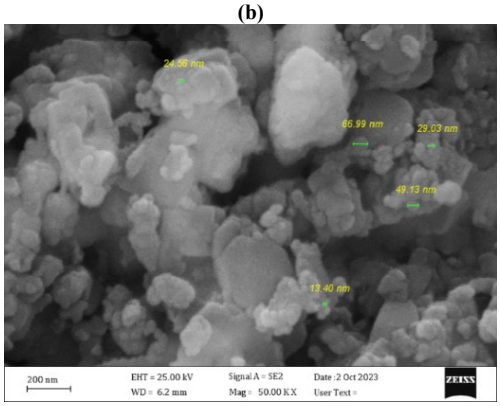

(c)

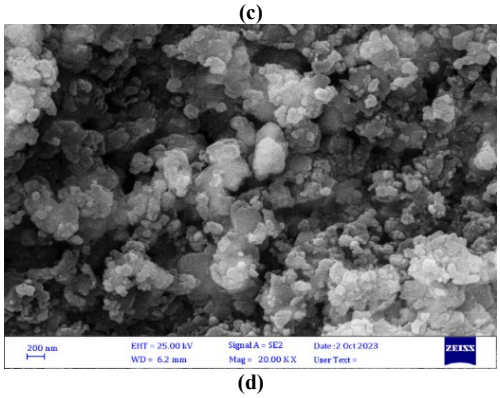

(d)

Fig. (8) (a-d) FE-SEM images of the sliver (Ag) NPs preparation by the Touilodin Blue (TB) dye powder by the hydrothermal method

The EDX spectrum is mainly used for identifying the elemental composition, and purity of the biogenic synthesized Ag nanoparticles, as shown in Fig. (9). A

strong signal for Ag, with high atomic percent values, was noted at 2 keV, which confirms the formation of lemons extract synthesized chemical method. Additionally, a few weak signals of C, N, Na, Au, and S were also obtained, attributed to the existence of plant bioactive molecules that are linked to the surface of the Ag nanoparticles. As shown in Fig. (9b), the image pattern of the biosynthesized Ag NPs of limon juice extract was mainly characterized using EDX micrographs. The same result was reported in some previous study. As illustrated in Fig. (9b), the EDX spectrum is primarily utilized to determine the elemental composition and purity of biogenic produced Ag nanoparticles. At 2 keV, a significant Ag signal with high atomic percent values was seen, confirming the production of Ag nanoparticles produced with an aqueous extract of lemon juice extract. A few faint signals of C, N, Na, Au, and S were also observed, which was attributed to the presence of plant bioactive molecules connected to the surface of the Ag nanoparticles.

The EDX spectrum is primarily utilized to detect the elemental composition and purity of biogenic produced blue dye, as illustrated in Fig. (9c). A significant blue dye signal with high atomic percent values was seen at 2 keV, confirming the production of dyes produced via chemical method. In addition, a few faint signals of C, O, Na, Au, and S were observed, which was attributed to the presence of blue dye [9].

The EDX spectrum is largely used to determine the elemental composition and purity of biogenic Ag nanoparticles, as shown in Fig. (9d). At 2 keV, a strong Ag signal with high atomic percent values was seen, demonstrating the formation of Ag nanoparticles from a blue dye. In addition, a few modest C, O, and Au, signals were detected, which was attributed to the existence of dye bioactive molecules attached to the surface of the Ag nanoparticles.

The transmission electron microscopy (TEM) carried out to investigate the morphology of prepared samples, using transmission electron microscopy type (Thermoscientific Quattro S). The typical transmission electron microscope images and histogram of the synthesized nanoparticles are presented in Fig. (10). The TEM images demonstrated that the synthesized of H, G, F and E samples were dispersed generally spherical in shape and well-formed nanoparticles. From Fig. (10H), the pure silver nanoparticles Ag nanoparticles (H) showed spherical nanoparticles detected in the range of 30-130 nm with average diameter about 52 nm as explained at the opposite TEM image of H sample, with a little aggregation of Ag nanoparticles. After the adding of lemon observed that the obtained nanoparticles with almost spherical shape detected at the range 10-130 nm with average diameter about 64 nm as presented at the opposite TEM image of G sample, with higher aggregation Ag nanoparticles compared with the sample without lemon, as shown in Fig. (10G).

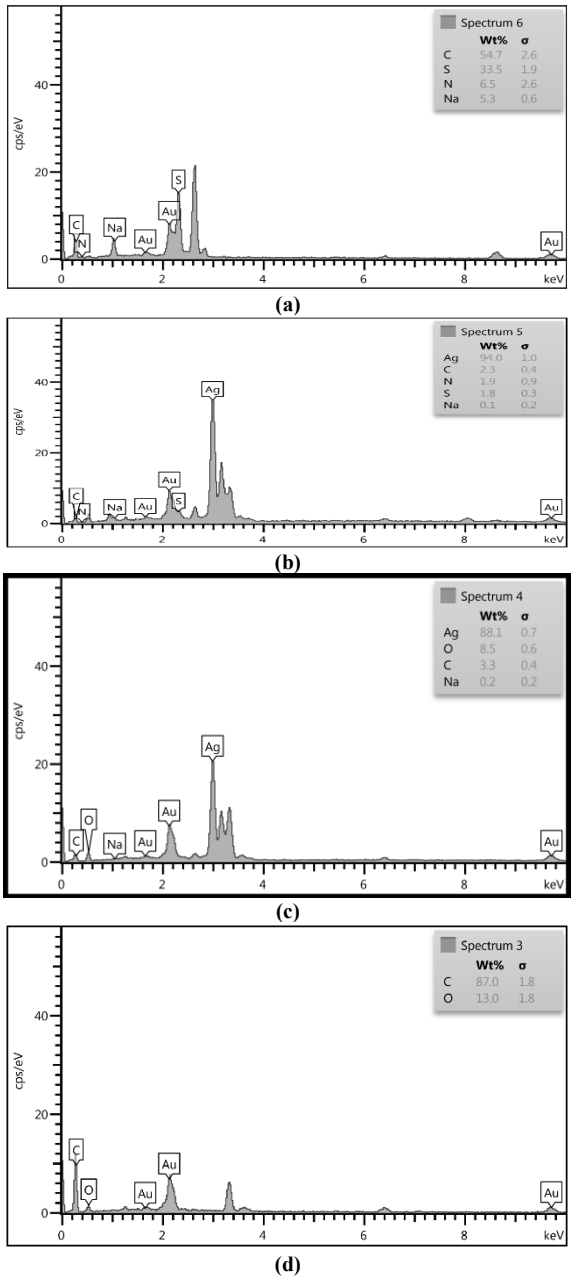

Fig. (9) EDX spectra of (a) lemons juice extract preparation by chemical method, (b) Ag-lemons juice extract preparation by chemical method, (c) blue dye powder, and (d) Ag nanoparticles preparation from lemon juice

While the TEM results of the Ag nanoparticles with added toluidine blue exhibited clear differences compared to those Ag nanoparticles without toluidine, observed clear aggregation of the Ag nanoparticles, these arrangements were several hundred nanometers wide and composed of hundreds of adjacent Ag nanoparticles, although there were still large numbers of Ag nanoparticles scattered singly and in small clusters. As showed in Fig. (10F). The spherical shape

Ag nanoparticles detected at the range 30-110 nm with average diameter about 55 nm, as shown at the opposite TEM image of F sample.

The TEM image of Ag nanoparticles with the adding of lemon and stain, It was observed that the silver nanoparticles Ag nanoparticles are generally spherical in shape, and there are a large number of individually dispersed Ag nanoparticles, in addition to some large agglomerations of these nanoparticles with micrometer diameters, this huge aggregation of Ag nanoparticles can be attributed to toluidine blue, due to the anionic strength of the sample solution, in addition to the charges on the stain that can be an important factor because the electrostatic repulsion or attraction. The spherical shape Ag nanoparticles observed at the range 50-130 nm with average diameter about 70 nm, as showed at the opposite TEM image of E sample.

The current study, in general, reveals that Touilodin Blue Dye and lemon juice extract act as good reducing and stabilizing agents in the synthesis of silver nanoparticles. Likewise, it is shown that the silver nanoparticles exhibit improved crystallinity and enhanced optical properties. Further studies must be aimed at fine-tuning the synthesis parameters so that the properties of the nanoparticles can be tuned according to a particular application. Finally, scaling up the method and checking for the applicability in practice are also required according to the results of recent studies on scalability.

4. Conclusion

The synthesized Ag nanoparticles possessed an f.c.c. structure and lemon juice improved its crystallinity and stability. A characteristic plasmon resonance band confirmed the successful formation of nanoparticles and their possible utility in optical applications. The natural functional groups, including -NH, -CO, and -OH, were involved in the reduction and stabilization mechanisms. The Ag nanoparticles had a uniform semi-spherical shape, which is of utmost importance in various applications. These results, which use natural extracts in the synthesis of silver nanoparticles, open avenues for much more sustainable and green technological developments. The results of this study are the stepping stone to further innovative steps in green nanotechnology, focusing on the integration of natural ingredients for rendering properties to nanomaterials and applications.

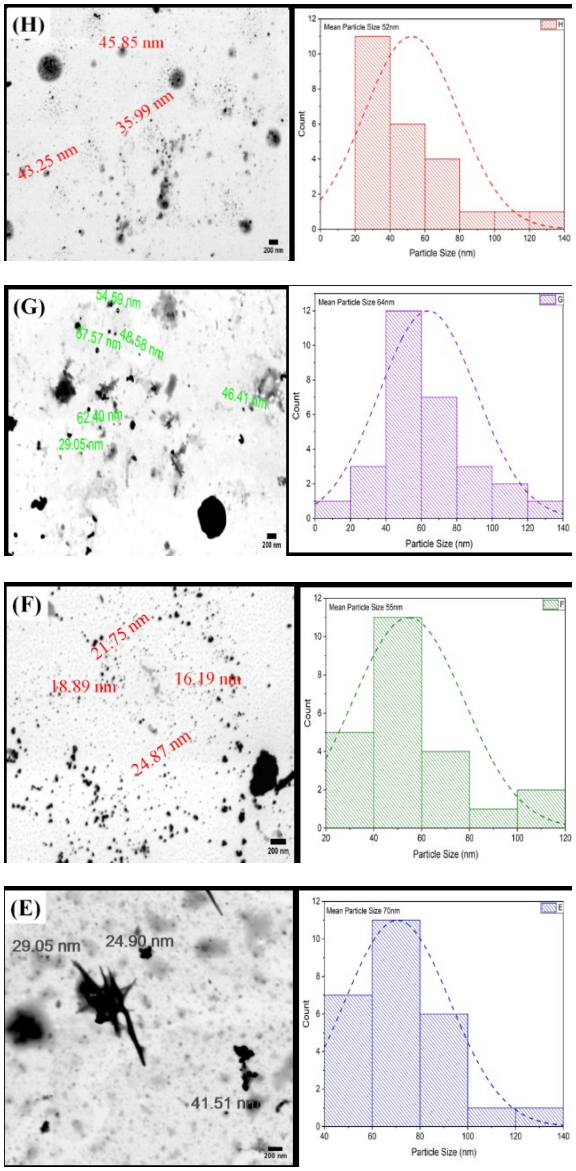

Fig. (10) TEM images of synthesized nanoparticles (H) Ag nanoparticles (G) Ag nanoparticles @ lemon (F) Ag nanoparticles @ stain (E) Ag nanoparticles @ lemon @ stain

References

[1] J. Doe et al., "Application of silver nanoparticles in medical devices and water treatment: A review", *J. Nanoparticle Res.*, 18(1) (2022) 123-137.

[2] B.C. Smith and D.E. Wilson, "Environmental impacts of nanomaterial production: Challenges and perspectives", *Enviro. Sci. Technol.*, 55(3) (2021) 400-415.

[3] L. Zhao et al., "Green synthesis of nanoparticles: Current developments and limitations", *Renew. Sustain. Ener. Rev.*, 41 (2020) 1573-1580.

[4] M. Taylor and N. Brown, "Plant extracts as natural reducing agents for nanoparticle synthesis: A review", *J. Clean. Product.*, 250 (2019) 1197-1210.

[5] G. White and H. Khan, "Citric acid as a reducing agent for biosynthesis of silver nanoparticles", *ACS Sustain. Chem. Eng.*, 8(6) (2018) 5203-5210.
[6] K. Lee et al., "Controlled synthesis of nanoparticles using laser irradiation: Towards smart nanoparticle fabrication", *Adv. Mater. Interfaces*, 7(14) (2021) 2000341.
[7] F. Johnson and A. Patel, "Innovations in laser-assisted nanoparticle synthesis", *Mater. Sci. Eng. R: Reports*, 139 (2020) 1-22.
[8] G.E.J. Poinern et al., "Green biosynthesis of silver nanocubes using the leaf extracts from Eucalyptus macrocarpa", *Nano Bull.*, 2(1) (2013).
[9] B. Das et al., "Green synthesized silver nanoparticles destroy multidrug-resistant bacteria via reactive oxygen species mediated membrane damage", *Arabian J. Chem.*, 10(6) (2017) 862-876.
[10] M. Kahloul et al., "Interaction of toluidine blue dye with heptamolybdate: UV–visible and ultrafiltration study", *Enviro. Develop. Sustain.*, 22 (2020) 4655-4672.
[11] U.M. Chougale et al., "Synthesis, characterization and surface deformation study of nanocrystalline Ag_2Se thin films", *Mater. Phys. Mech.*, 17(1) (2013) 47-58.
[12] K.L. Penniston et al., "Quantitative assessment of citric acid in lemon juice, lime juice and commercially-available fruit juice products", *J. Endourol.*, 22 (2008) 567–570.
[13] H. Qiu et al., "Critical review in adsorption kinetic models", *J. Zhejiang Univ. Sci. A*, 10(5) (2009) 716–724.
[14] B. Saha et al., "Comparative study of toluidine blue O and methylene blue binding to lysozyme and their inhibitory effects on protein aggregation", *ACS Omega*, 3(3) (2018) 2588-2601.
[15] M.J. Hakeem et al., "Role of salts and solvents on the defibrillation of food dye 'sunset yellow' induced hen egg white lysozyme amyloid fibrils", *Int. J. Biol. Macromol.*, 219 (2022) 1351-1359.
[16] R. Gnanasambandam and A. Proctor, "Preparation of soy hull pectin", *Food Chem.*, 65 (1999) 461–467.
[17] M.T. Kartel, L.A. Kupchik and B. K. Veisov, "Evaluation of pectin binding of heavy metal ions in aqueous solutions", *Chemosphere*, 38 (1999) 2591–2596.
[18] J.F. Kefford and B.W. Chandler, **"The Chemical Constituents of Citrus Fruits"**, Academic Press (NY, 1970).
[19] Y. Khane et al., "Green synthesis of silver nanoparticles using aqueous Citrus lemon zest extract: Characterization and evaluation of their antioxidant and antimicrobial properties", *Nanomater.*, 12(12) (2012) article no. 2013.
[20] I.A. Fadhil et al., "Influence of Adding Silver Nanoparticles on Structural and Optical Characteristics of PMMA Nanopowders for Antibacterial Applications", *Iraqi J. Appl. Phys.*, 21(2) (2025) 286-290.
[21] M.H. Al-Janabi, Ç.Y. Ataol and A. Ramizy, "Characterization of Silver Nanoparticles Prepared by Cold Plasma Reaction", *Iraqi J. Appl. Phys.*, 20(2A) (2024) 279-284.
[22] B.C. Smith, "Crystallinity in silver nanoparticles synthesized with synthetic reductants", *Mater. Sci. Eng. R: Reports*, 139 (2021) 58-72.
[23] L. Zhao et al., "Phytochemicals in green synthesis of nanoparticles", *ACS Sustain. Chem. Eng.*, 9(4) (2020) 1526-1542.
[24] M. Taylor and N. Brown, "Impact of organic constituents on the nucleation and growth of nanoparticles", *J. Clean. Product.*, 250 (2019) 1197-1210.
[25] G. White and H. Khan, "Comparative study of stabilization mechanisms in nanoparticle synthesis", *Chem. Rev.*, 118(18) (2018) 5392-5422.
[26] K. Lee et al., "Optical properties of biologically synthesized nanoparticles", *Adv. Mater. Interfaces*, 7(14) (2021) 2000341.
[27] F. Johnson and A. Patel, "Applications of nanoparticle optical properties in medical therapy", *Nano Today*, 15 (2022) 81-92.
[28] H. Greene and I. Khan, "Functional groups in nanoparticle synthesis", *Nanotech.*, 12(1) (2019) 75-88.
[29] N. Saikia, "Inorganic-Based Nanoparticles and Biomaterials as Biocompatible Scaffolds for Regenerative Medicine and Tissue Engineering: Current Advances and Trends of Development", *inoragnics*, 12(11) (2024) 292.
[30] S. Ahmad et al., "Stability and dispersion of silver nanoparticles", *Phys. Chem. Chem. Phys.*, 21(7) (2021) 10342-10352.
[31] U. Ulusoy, "A Review of Particle Shape Effects on Material Properties for Various Engineering Applications: From Macro to Nanoscale", *minerals*, 13(1) (2023) 91.
[32] D.V. Leff, L. Brandt and J.R. Heath, "Synthesis and characterization of hydrophobic, organically-soluble gold nanocrystals functionalized with primary amines", *Langmuir*, 12(20) (1996) 4723-4730.
[33] S.L. Westcott et al., "Formation and adsorption of clusters of gold nanoparticles onto functionalized silica nanoparticle surfaces", *Langmuir*, 14(19) (1998) 5396-5401.

Table (1) Results of crystallite size, dislocation density, and the microstrain for TB Dye, Ag-TB Dye, Ag-lemons

Phases	Temperature (°C)	2θ Exp. (deg)	2θ JCPDS (deg)	FWHM (deg)	(hkl)	Crystallite size D (nm)	Dislocation density (line/m^2)x10^{15}	Micro Strain x10^{-3}
TB	Standard	25.8	25.9	0.58	(002)	13.980	51.164	24.784
		27.7	27.8	0.54	(100)	15.076	43.997	22.983
		31.3	31.4	0.89	(101)	9.224	117.525	37.563
		46.1	46.7	0.69	(102)	12.482	64.181	27.759
		56.8	56.4	0.46	(103)	19.514	26.260	17.756
		76.7	76.9	0.59	(104)	13.942	51.440	24.851
Ag-TB	200	38.4	38.9	0.28	(111)	29.165	11.755	11.880
		44.3	44.7	0.12	(100)	71.139	1.9759	4.870
		64.2	64.7	0.25	(200)	37.223	7.217	9.308
		77.7	77.9	0.28	(240)	33.249	9.045	10.421
Ag-lemons		38.3	38.4	0.76	(111)	11.020	31.440	82.333
		44.1	44.4	0.87	(100)	9.812	35.312	103.862
		64.1	64.3	0.97	(200)	9.685	35.773	106.589
		77.1	77.8	0.95	(240)	10.709	32.353	87.181

